AFAPL-TR-69-113, Pt. VI, Feb. 1970, Air Force Propulsion Lab., Wright-Patterson Air Force Base, Ohio.

[3] Tjonneland, E. and O'Neill, E. B., "Total Pressure Turbulence in a Sharp Lip Axisymmetric Supersonic Intake Operating in the Flowfield of an Airplane Wing and Flap System in Takeoff Configurations," AIAA Paper 68-50, Jan. 22–24, 1968, New York, N.Y.

[4] Przybylko, S. J., Hutcheson, L., Suder, B., and Warwick, T. R., "Advanced Integrated Digital Engine Simulation," AIAA Paper 70-633, San Diego, Calif., June 1970.

[5] Kulberg, J. F., Shepard, D. E., King, E. O., and Baker, J. R., "Dynamic Simulation of Turbine Engine Compressor," AIAA Paper 69-486, June 9–13, 1969, U.S. Air Force Academy, Colo.

[6] Cotter, H. N., "Integration of Inlet and Engine—An Engine Man's Point of View," SAE Paper 680286, April 1968.

[7] Plourde, G. A., and Brimelow, B., "Pressure Fluctuations Cause Compressor Instability," Airframe/Propulsion Compatibility Symposium, June 1969, Air Force Aero Propulsion Lab., Air Force Flight Dynamics Lab., Wright-Patterson Air Force Base, Ohio.

MAY 1971 J. AIRCRAFT VOL. 8, NO. 5

Development of High-Response Data Analysis AIDS for Inlet-Engine Testing

MALCOLM ROWE* AND MARK B. SUSSMAN*
The Boeing Company, Seattle, Wash.

The paper describes two data analysis aids recently developed to provide easy interpretation of high-response inlet flowfield information. A light bulb display is utilized as an analog simulation of the engine compressor face. Bulbs, on a one-to-one basis with high-response pressure transducers, provide flow visualization of high-frequency (to 1000 Hz) pressure fluctuations. A second analog device instantaneously sums the inputs of a select number of compressor face probes. Its output signal is used as an index to establish the degree to which the compressor face pulsations are one dimensional. Data from a recently conducted inlet-engine test program are used to illustrate the operation of both devices.

Nomenclature

A_{BY} = bypass door flow area (in.^{2})
A_L = area of circle with diameter equal to that of the cowl lip (in.^{2})
f = frequency (Hz)
f_p = pulsator frequency (Hz)
M_O = tunnel Mach number
$N/\theta^{1/2}$ = engine corrected speed (% of maximum)
P_{T2} = compressor face total pressure (psia)
P_{TO} = tunnel total pressure (psia)
S_{IND} = summation index = R_{SN}/S_{RN} (see Appendix)
T_{TO} = tunnel total temperature (°F)
α = angle of attack (degrees)

1 Introduction

RECENT experience with supersonic aircraft has exposed several serious propulsion system problems. Specifically considered here are those concerning inlet/engine compatibility.

Compressor stall difficulties encountered during ground and flight testing of two recent aircraft systems have been reported upon by Rall.[1] Numerous other references exist. The source of these stall difficulties has been the quality of air presented to the engine. Because of these difficulties, many test data have been accumulated recently bearing on the condition of the air delivered by the inlet. The flow properties of the air are generally expressed in terms of distortion and turbulence characteristics. These two words are not always used uniformly, but the definitions used here are consistent with current instrumentation practices: "Distortion" is spatial nonuniformity in total pressure as measured by very slow response (e.g., manometer tube) instrumentation; and "turbulence" is transient activity of the compressor-face flow as measured by high-response (d.c. to 10,000 Hz) instrumentation. This may include the condition of distortion when the pattern is rapidly changing in time or pulsation when the spatial field moves in phase.

The degree to which the engine will withstand poor-quality air has also been the subject of investigation. Conclusions based on these diverse data have not always been unanimously accepted. This is readily attributed to the general lack of understanding concerning precisely how the engine is affected by the quality of air entering it. To date, theoretical foundations upon which to build this understanding are limited. Current understanding therefore rests largely on experimental data.

Thus, today, several distinctly different theories are advanced by separate investigators concerning compressor stall problems. At least three are readily identifiable; the major assertions of each are described below.

1) According to the first theory, the compressor is primarily sensitive to distortion patterns. This sensitivity extends to the case when these distortion patterns are changing rapidly in time. Thus, this theory asserts that turbulence, as defined here, is simply time-varying distortion.

2) A second theory for explaining the effect of nonsteady airflow on the operation of an engine has been suggested by a test that was run at AEDC, in which a J93 engine was operated behind a simulated inlet or "turbulator." From the results of this test, it was concluded that the reduction in surge margin of an engine can be correlated with the root-mean-square (rms) level of the time-varying component of the total pressure at the compressor face.

In this approach, based on a statistical theory, it is assumed that the most significant parameter of the nonsteady flow is

Received December 12, 1969; revision received April 20, 1970. Sponsored by Air Force Flight Dynamics Laboratory (AFSC), Dennis Sedlock, AFFDL Project Engineer, Contract F33657-69-C-0552. The authors are very happy to thank numerous Boeing engineers for their contributions to this paper.

* Specialist Engineer, Propulsion Staff, Commercial Airplane Group. Member AIAA.

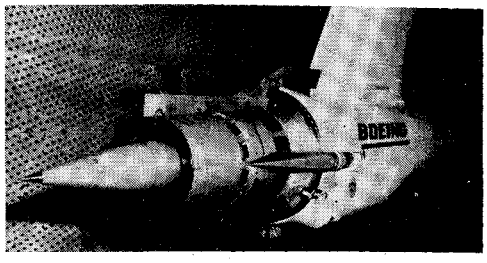

Fig. 1 Inlet-engine installation.

the average level of pressure fluctuations or turbulence experienced by the engine, and that this turbulence has the effect of reducing the surge-pressure ratio of the engine.

3) The third theory considers that, in a dynamic sense, the inlet flowfield may not be what is predicted, based on a steady-state analytical model. Specifically envisioned are possible large-order pulsations of the flow. These may be partly or, perhaps, completely correlated over the compressor face. In any event, this line of reasoning associates particular discrete frequencies with a given inlet/engine configuration. It is believed that flow transients detrimental to system stability would occur, then, at these rather low (and predictable) "acoustic" frequencies.

In view of the limited theoretical framework and consequent high reliance upon experimental data, it is necessary that this data be carefully analyzed. Previous experience with conventional steady-state instrumentation has proven the value of such data analysis aids as flow visualization. The increased physical understanding of the flowfield provided by such techniques has often led to improved analytical models.

This paper describes two test techniques used in a supersonic inlet-turbojet engine compatibility test conducted in the 16T Propulsion Wind Tunnel at AEDC, Tullahoma, Tenn. during August 1969. The first technique uses a panel of lights to indicate the flow fluctuations over the interface plane (the compressor face) between the inlet and the engine. Electrical signals from pressure transducers in this plane on the test model are slowed down and made to illuminate light bulbs geometrically arranged on the (remote) panel at positions corresponding to the transducers. The second technique involves measuring the degree with which the flow at the compressor face is one-dimensional over a period of time. This is achieved by evaluating the root mean square value of the instantaneous sum of the signals from the compressor face transducers.

The paper is organized in the following manner. First, a brief description of the wind-tunnel test is presented. Then, the specific purpose and function of both the light panel and the Summation Device analysis aids are presented separately. Experience using these aids during the test is discussed, and film sequences with the light panel are included. These illustrate surge and rotating stall behavior at the compressor face.

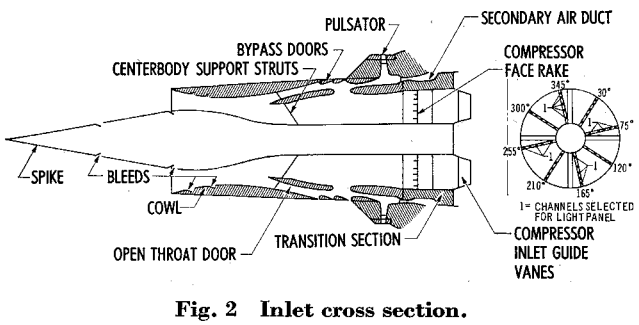

Fig. 2 Inlet cross section.

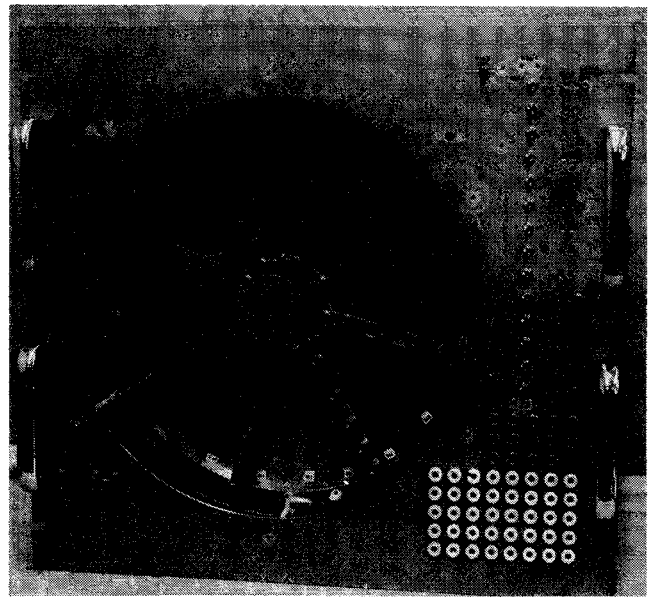

Fig. 3 Light panel with light diffusing screen removed.

2 Description of the Wind-Tunnel Test

The test program was conducted under U.S. Air Force sponsorship in August 1969, in the 16-ft Transonic Propulsion Wind Tunnel (PWT-16T) at the Arnold Engineering Development Center, Tullahoma, Tenn. The basic purpose of the test was to provide information relating to the design and development of inlet-engine propulsion systems. The inlet is an axisymmetric, translating spike, mixed compression 0.255 scale model of an early supersonic transport concept. The cowl-lip diameter is 16.28 in. The inlet was coupled by a short transition section to either a General Electric J85 turbojet engine or a cold-flow duct, strut mounted from the ceiling of the tunnel (Fig. 1). A cross section of the inlet is shown in Fig. 2.

Compressor surge could be induced on command by injecting air from a high-pressure supply to engine customer bleed ports. Definition of the surge line using this technique has been demonstrated to be in good agreement with the more conventional technique of nozzle closure.

To assess inlet resonance phenomena, discrete-frequency pressure variations at the compressor face were introduced by the pulsator noted in Fig. 2. This pressure disturbance system generates pressure waves within the inlet by rapidly varying the amount of air channeled through the secondary air system. It consists of a rotating ring having 60 slots passing over a fixed ring with similar slots. Rotating the outer ring at 200 rpm causes pulsations at 200 Hz.

The test configuration was highly instrumented in terms of both steady state and high-response pressure sensors. Of interest here are the rakes of total pressure probes at the compressor face. As shown to the right of Fig. 2, there are

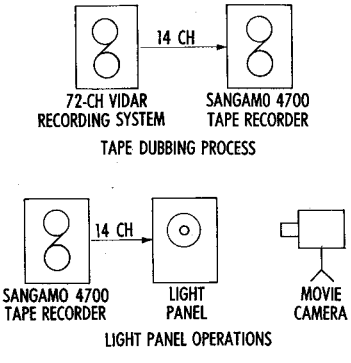

Fig. 4 Tape dubbing process and light panel operation.

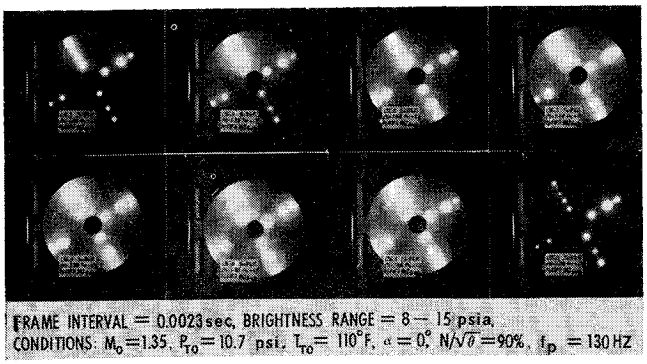

Fig. 5 Compressor face pressures during engine surge.

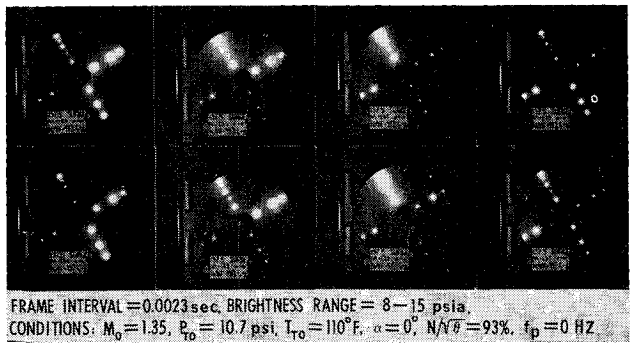

Fig. 6 Compressor face pressures during rotating stall.

8 rakes each having 5 probes. A Kulite XPLB-093-50A transducer was flush mounted in each probe and protected from particle damage by a Boeing designed windscreen.

Low-frequency (d.c. to 1000 Hz) pressure fluctuations were recorded on a 78-channel VIDAR data acquisition system. Fourteen of these channels were selected for replay to the light panel (see Fig. 2). High-frequency (1 Hz to 10 kHz) data were recorded on a separate 32-channel turbulence, wide-band FM tape recording system. Sixteen of these high-frequency channels representing data from the second and fourth transducer on each rake were routed directly to the Summation Device.

3 Light Panel Display

The light panel was constructed to provide a visual representation of the compressor face total pressures within a short time of the completion of a test run. Visualization was achieved by playing the tape-recorded pressure signals back at a slower speed through the light bulbs.

The panel is shown with the light diffusing screen removed in Fig. 3. It consists of 8 rakes of 5 light bulbs each (6.3v instrumentation lamps) located at corresponding positions in the panel "annulus" as were the rakes and pressure transducers at the compressor face of the actual inlet model. The dimensions of the panel annulus are approximately the same as those of the inlet model. To allow for different probe configurations, the panel rakes could be moved to any of 24 locations at 15° intervals around the annulus. In order that the pressure fluctuations cause a reasonable fluctuation in light intensity within the operating range of the bulbs, the light panel channels include a d.c. amplifier (Preston Model 704) and an adjustable bias circuit.

The panel was operated as indicated by Fig. 4. Tape recorder availability limited the number of operating channels to 14. Selected runs from a night's testing were dubbed at a slower speed from the test data tape on the 72-channel Vidar recording system to a second magnetic tape on a Sangamo 4700 tape recorder. The dubbed data were then played through the light panel, again at a slower speed. The various tape speeds were as indicated in Table 1.

The total speed reduction was 128 times. A 16mm movie was then made of the resulting display. Data identification on the Vidar was made using an IRIG "B" time code in conjunction with an oscillograph strip-out. Data identification on the Sangamo tape was by voice, recorded on an edge track at 1-$\frac{7}{8}$ in./sec.

Although it was possible to adjust the bias setting for each channel so that a particular brightness corresponded to a known pressure level, and adjust the amplifier gain to optimize the brightness variation for a particular event (e.g., buzz or surge), it was found impractical on this occasion to do this in the limited time available between tests. As a compromise, the biases were adjusted so that for runs with the inlet model at zero angle-of-attack and steady-flow conditions, the bulbs were about half-way through their brightness range (2–6.3v). Likewise, a compromise gain setting was chosen, so that a change from minimum to maximum bulb brightness was caused by a pressure rise of about 7 psi. Bulb burn-out was prevented by setting a potential divider between the amplifier output and the corresponding bulb; so that the amplifier saturation voltage put a voltage across the bulb slightly less than the burn-out voltage. A pressure fluctuation of approximately 0.5 psi was just discernible to the eye at a midrange-mean bulb brightness.

Using the light panel, it was possible to judge the relative effects of pulsator, buzz and surge on the flow at the compressor face simultaneously at a number of points in the annulus cross section. Little radial variation in the flow fluctuations for any of these phenomena was observed. Some rotating stall (rotating at about half the rpm) was clearly visible during a period while the engine was intermittently surging. Figure 5 shows a sequence of pictures of the light panel display illustrating the compressor face pressure distribution during engine surge. The brightness range is from about 8 psia (lights just on) to 15 psia (maximum brightness). In this particular example, the inlet was at zero angle-of-attack and the tunnel-flow conditions were: M_O = 1.35, P_{TO} = 10.7 psia, T_{TO} = 110°F. The engine corrected speed was 90% of its maximum value, and the pulsator was set at 130 Hz (it induced pressure fluctuations of about 1 psi at the compressor face). Surge was induced by increasing the reverse bleed flow.

Table 1 Tape-recorder speeds in./sec

Vidar record speed	60
Vidar playback speed	15
Sangamo record speed	60
Sangamo playback speed	1$\frac{7}{8}$

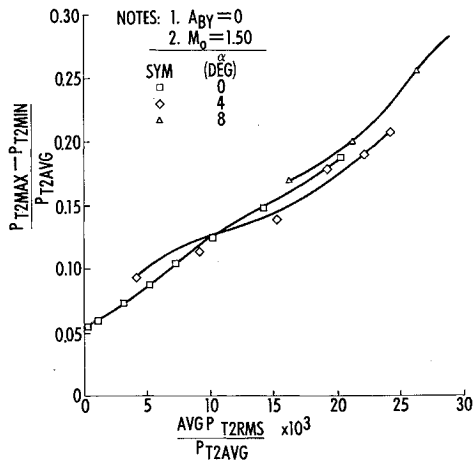

Fig. 7 Compressor face flow distortion vs rms for inlet and cold-flow duct.

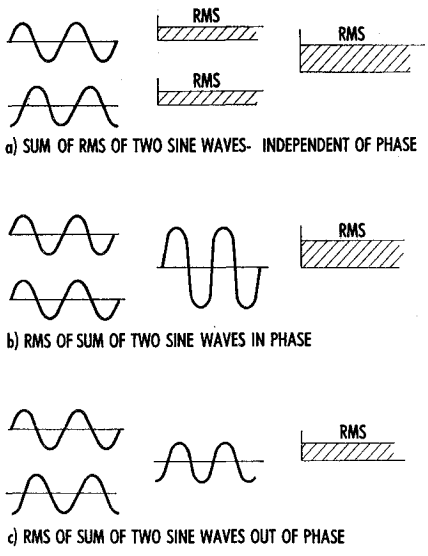

Fig. 8 Principle of summation device.

Figure 6 shows a sequence of light panel pictures during rotating stall. This was observed following a similar surge to that shown in Fig. 5, except that the engine corrected speed was 93% of its maximum value (actual engine speed was 16,060 rpm), and the pulsator frequency was zero.

4 Summation Device

Average compressor face rms levels have been widely used to correlate the degree of "badness" of inlet flowfields. This is more because of the ease of obtaining the number than because of its effectiveness. In fact, surge margin correlations against rms indicators tend to have considerable scatter.[2] That is, at a given rms level, the engine will surge under some conditions but not others.

Furthermore, simply as a gauge of inlet flow conditions, without worrying about engine effect, the rms level will often correlate quite well against the steady-state distortion level as seen, i.e., in Fig. 7. We have observed that for fixed inlet geometry, such a correlation is often achieved, being indicative of normal inlet flow. We have supposed that for some inlet flow conditions, flow fluctuations occur which contribute to the over-all rms level but which must be further distinguished. Under the additional assumption, that these other fluctuations are well-correlated, and nearly one-dimensional at the compressor face, a summation index has been devised. The purpose of this index is to alert the data analyst to "in-phase" (or one-dimensional) fluctuation activity at the compressor face.

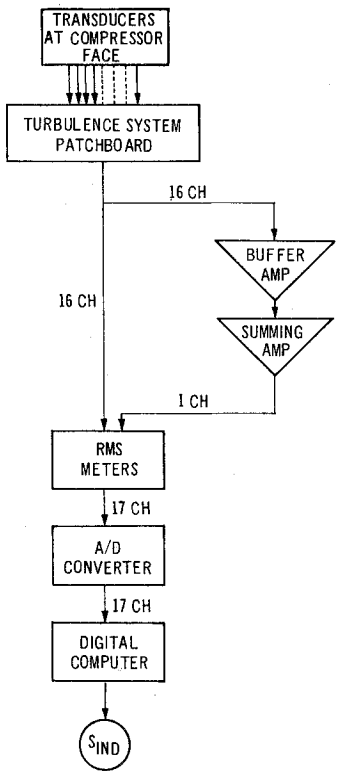

Fig. 9 Summation device block diagram.

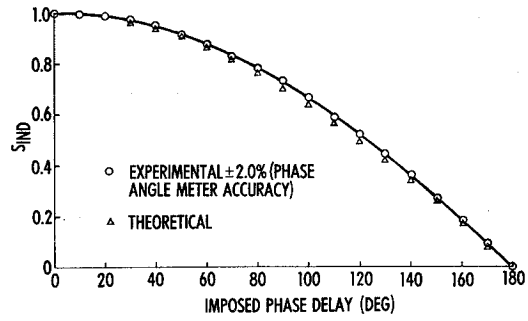

Fig. 10 Results of summation device checkout test.

The summation index concept is quite simple and based on the fact that if a number of transducer outputs are summed and then put through a rms meter, the value obtained will be different than if the outputs are led through individual rms meters and then summed. The two values will differ proportionally to the degree which the transducer outputs are out of phase. The situation is illustrated schematically in Fig. 8. Case A shows the sum of the rms levels obtained from two-sine waves. The value obtained is independent of the phase difference between the sine waves. Case B shows the rms level obtained from the sum of two-sine waves in phase. The final value is the same as in case A. Case C shows the rms level obtained from two-sine waves which are out of phase. This value is less than the values for cases A and B. A mathematical discussion is contained in the Appendix. The summation index S_{IND} is defined as the ratio of the rms of the sum of N signals R_{SN} to the sum of the individual rms values of N signals S_{RN}.

Of course this same information can be obtained through joint correlation analyses of compressor face probe pairs. However, the Summation Device described below has been developed as an attempt to simply and rapidly obtain this information on-line.

A block diagram illustrating usage of the Summation Device (SD) is shown in Fig. 9. For the test discussed in this paper, the device was set up to accept 16 compressor face data channels. Each of the 16 channels was first led through a "buffer" amplifier in order to protect the rest of the data acquisition system from any failure of the SD. These signals were then led through a summing amplifier whose output was then passed through an rms meter, sampled and acquired through the on-line data reduction computer. In addition, the SD output signal was recorded on tape for later analysis.

Results of a simple checkout test performed after fabrication of the device are shown in Fig. 10. For this test, a 200-Hz sine wave was impressed on 16-input channels. Eight of these were led directly into the Summation Device. The remaining group of eight were routed through a variable-phase-delay black box prior to being input to the SD. The value of the Summation Index was obtained as a function of the imposed phase delay. As desired, the Summation Index uniformly approaches zero as the phase difference approaches 180°, following the predicted cosine variation.

Additional properties of the Summation Device are frequency response characteristics as follows: amplitude re-

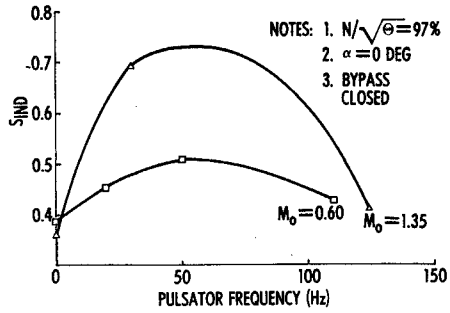

Fig. 11 Summation index vs pulsator frequency.

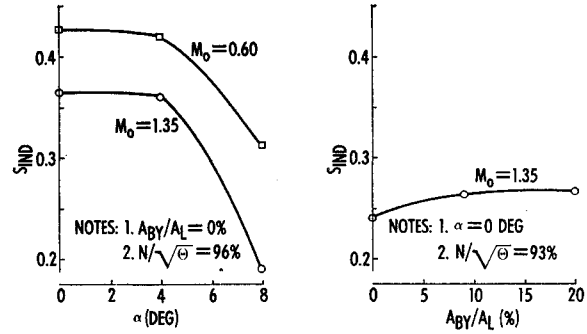

Fig. 12 Summation index trend with angle of attack and bypass door setting.

sponse—flat ± 1 db, 1–20,000 Hz and phase lag—4° at 10,000 Hz.

Figure 11 illustrates results obtained during the inlet-engine test previously described. The Summation Index is plotted as a function of pulsator frequency for two different Mach numbers. The corrected engine speed is 97% for all points. It is seen that for zero pulsator speed (pulsator off), the ordinate is quite small, indicating very little in-phase (i.e., one-dimensional) activity. As the pulsator speed is increased, a large degree of in-phase activity is shown (as expected). At still higher frequencies, the pulsator is producing a smaller amplitude disturbance.

Figure 12 is typical of some of the data trends which were established based on the on-line data output. In Fig. 12a the variation with α is quite flat initially, but shows a large fall off in the degree of in-phase compressor face activity at large α. The trend is maintained at both subsonic and supersonic Mach numbers and is in agreement with an intuitive picture of increasingly erratic flow at angle-of-attack. The trend with bypass door position in Fig. 12b is not so pronounced, but indicates an increasing level of correlation at the compressor face with increasing amounts of bypass. These trends must be more fully evaluated in the future in order to obtain experience regarding the range and scatter associated with numerical values of the ordinate scale.

Appendix

Theory of Summation Device

Consider N channels of data $x_1(t) \ldots x_N(t)$. The rms of a typical channel $x_k(t)$ is defined by

$$\text{rms}(x_k) = \left\{ \lim_{T\to\infty} \frac{1}{T} \int_0^T [x_k(t)]^2 \, dt \right\}^{1/2}$$

Suppose each signal can be represented by a sine series. Thus, e.g.,

$$x_k(t) = a_{1k} \sin(t + \phi_{1k}) + a_{2k} \sin(2t + \phi_{2k}) + \ldots + a_{nk} \sin(nt + \phi_{nk}) + \ldots$$

then

$$\text{rms}(x_k) = \left\{ \lim_{T\to\infty} \frac{1}{T} \int_0^T [a_{1k} \sin(t + \phi_{1k}) + a_{2k} \sin(2t + \phi_{2k}) + \ldots \quad + a_{nk} \sin(nt + \phi_{nk}) + \ldots]^2 \, dt \right\}^{1/2}$$

$$= \left\{ \frac{1}{2\pi} \int_0^{2\pi} a_{1k}^2 \sin^2 t \, dt + \frac{1}{\pi} \int_0^{\pi} a_{2k}^2 \sin^2 2t \, dt + \ldots + \frac{n}{2\pi} \int_0^{2\pi/n} a_{nk}^2 \sin^2 nt \, dt + \ldots \right\}^{1/2} = \frac{1}{(2)^{1/2}} \left(\sum_{n=1}^{\infty} a_{nk}^2 \right)^{1/2}$$

The sum of the rms values of N channels, denoted by S_{RN}, is thus given by

$$S_{RN} = \frac{1}{(2)^{1/2}} \sum_{k=1}^{N} \left(\sum_{n=1}^{\infty} a_{nk}^2 \right)^{1/2}$$

The rms value of the sum of N channels, denoted by R_{SN}, is given by

$$R_{SN} = \left\{ \lim_{T\to\infty} \frac{1}{T} \int_0^T [x_1(t) + x_2(t) + \ldots + x_N(t)]^2 \, dt \right\}^{1/2}$$

$$= \left\{ \lim_{T\to\infty} \frac{1}{T} \int_0^T \left[\sum_{k=1}^{N} \sum_{n=1}^{\infty} a_{nk} \sin(nt + \phi_{nk}) \right]^2 dt \right\}^{1/2}$$

The terms within the integral are made up of: 1) squares of terms such as $a_{nk} \sin(nt + \phi_{nk})$; 2) products of terms such as $a_{np} \sin(nt + \phi_{np})$ and $a_{nq} \sin(nt + \phi_{nq})$; and 3) products of terms such as $a_{np} \sin(nt + \phi_{np})$ and $a_{mq} \sin(mt + \phi_{mq})$.

Terms 1) contribute values $a_{nk}^2/2$ to $(R_{SN})^2$, terms 2) contribute values $(a_{np} \cdot a_{nq}/2) \cos(\phi_{np} - \phi_{nq})$ to $(R_{SN})^2$, and terms 3) make no contribution to $(R_{SN})^2$.

The maximum value of R_{SN} occurs when $\phi_{np} = \phi_{nq}$ for all values of p and q, i.e., when all the signals are in phase. Thus,

$$(R_{SN})_{\max} = \frac{1}{(2)^{1/2}} \left\{ \sum_{n=1}^{\infty} \sum_{k=1}^{N} a_{nk}^2 + \sum_{n=1}^{\infty} \sum_{\substack{p=1 \\ q=1}}^{N} {}_{p\neq q} \, a_{np} \cdot a_{nq} \right\}^{1/2}$$

Writing

$$\sum_{n=1}^{\infty} a_{nk}^2 = A_k^2 \text{ and } \sum_{n=1}^{\infty} a_{np} \cdot a_{nq} = A_p A_q,$$

$$(R_{SN})_{\max} = \frac{1}{(2)^{1/2}} \left\{ \sum_{k=1}^{N} A_k^2 + \sum_{\substack{p=1 \\ q=1}}^{N} {}_{p\neq q} \, A_p \cdot A_q \right\}^{1/2}$$

$$= \frac{1}{(2)^{1/2}} \left(\sum_{k=1}^{N} A_k \right) = \frac{1}{(2)^{1/2}} \sum_{k=1}^{N} \left(\sum_{n=1}^{\infty} a_{nk}^2 \right)^{1/2} = S_{RN}$$

It follows that $R_{SN} \leq S_{RN}$, i.e., the rms of the sum of N signals is less than or equal to the sum of the rms of N signals. Equality occurs when all the signals are in phase. A comparison of these two quantities will thus indicate the degree of in-phaseness of the set of signals, i.e., the extent to which the flow is one dimensional.

References

[1] Rall, F. T., "Aircraft and Propulsion Considerations Related to Inlet Design," AGARD Flight Mechanics Panel, Sept. 1967, Göttingen, Germany.

[2] Plourde, G. A., "Pressure Fluctuations Cause Compressor Instability," Paper presented at the Airframe Propulsion Compatibility Symposium, Miami Beach, Fla., June 1969.